Journal of Catalysis **189,** 52–62 (2000)
Article ID jcat.1999.2677, available online at http://www.idealibrary.com on IDEAL®

Perovskite-Type Halo-oxide $La_{1-x}Sr_xFeO_{3-\delta}X_\sigma$ (X = F, Cl) Catalysts Selective for the Oxidation of Ethane to Ethene

H. X. Dai, C. F. Ng, and C. T. Au[1]

Chemistry Department and Center for Surface Analysis and Research, Hong Kong Baptist University, Kowloon Tong, Hong Kong, China

Received May 4, 1999; revised August 4, 1999; accepted September 6, 1999

The catalytic performance and characterization of perovskite-type halo-oxide $La_{1-x}Sr_xFeO_{3-\delta}X_\sigma$ (X = F, Cl) as well as $La_{1-x}Sr_xFeO_{3-\delta}$ (x = 0–0.8) for the oxidative dehydrogenation of ethane (ODE) to ethene have been investigated. XRD results indicate that the catalysts had oxygen-deficient perovskite structures and TGA results demonstrated that the F- and Cl-doped perovskites were thermally stable. Under the reaction conditions of $C_2H_6/O_2/N_2$ = 2/1/3.7, temperature = 660°C, and space velocity = 6000 mL h^{-1} g^{-1}, C_2H_6 conversion, C_2H_4 selectivity, and C_2H_4 yield were, respectively, 55.3, 45.1, and 24.9% over $La_{0.6}Sr_{0.4}FeO_{3-0.048}$; 76.8, 62.1, and 47.7% over $La_{0.8}Sr_{0.2}FeO_{3-0.103}F_{0.216}$; and 84.4, 68.4, and 57.6% over $La_{0.6}Sr_{0.4}FeO_{3-0.103}Cl_{0.164}$. Over the two halo-oxide catalysts, with an increase in space velocity, C_2H_6 conversion decreased, whereas C_2H_4 selectivity increased. Both $La_{0.8}Sr_{0.2}FeO_{3-0.103}F_{0.216}$ and $La_{0.6}Sr_{0.4}FeO_{3-0.103}Cl_{0.164}$ were durable within 40 h of onstream ODE reaction. XPS results suggested that the presence of halide ions in the perovskite lattices promotes lattice oxygen mobility. It is apparent that the inclusion of F^- or Cl^- ions in $La_{1-x}Sr_xFeO_{3-\delta}$ can reduce the deep oxidation of C_2H_4 and thus enhance C_2H_4 selectivity. Based on the results of O_2-TPD and TPR studies, we suggest that the oxygen species that desorbed at temperatures ranging from 590 to 700°C over the $La_{0.8}Sr_{0.2}FeO_{3-0.103}F_{0.216}$ and $La_{0.6}Sr_{0.4}FeO_{3-0.103}Cl_{0.164}$ catalysts are active for the selective oxidation of ethane to ethene. By regulating the oxygen vacancy density and the oxidation states of B-site cations by implanting halide ions into oxygen vacancies in perovskite-type oxides (ABO_3), one may obtain catalysts that are durable and selective for the ODE reaction.

Key Words: **oxidative dehydrogenation; oxidative dehydrogenation of ethane reaction; ethane; ethene; perovskite; perovskite-type halo-oxides; $La_{1-x}Sr_xFeO_{3-\delta}$; $La_{1-x}Sr_xFeO_{3-\delta}X_\sigma$.**

INTRODUCTION

The oxidative coupling of methane (OCM) and the oxidative dehydrogenation of ethane (ODE) are two important reactions in the utilization of natural gas. As a secondary step in the OCM process, the ODE reaction has been intensively studied. Efforts have been focused on the development of tailormade catalysts. In addition to alkaline earth oxides (1, 2), rare earth oxides (3, 4), and transition metal oxides (5–7), perovskite-type oxides (ABO_3) have also been reported to be catalytically effective. After investigating the catalytic performance of $CaTi_{1-x}Fe_xO_{3-\delta}$ ($0 \le x \le 0.4$) and $SrTi_{1-x}Fe_xO_{3-\delta}$ ($0 \le x \le 1.0$) for the ODE reaction, Hayakawa *et al.* (8) found that the latter showed higher C_2H_4 selectivity than the former. Recently, they reported the catalytic activities of $SrFeO_{3-\delta}$ and $La_{1-x}Sr_xFeO_{3-\delta}$ ($0 \le x \le 1.0$) (9). At 650°C, with a C_2H_6/O_2 molar ratio of 1/1 and space velocity of 7000 mL h^{-1} g^{-1}, C_2H_6 conversion, C_2H_4 selectivity, and C_2H_4 yield were 87, 43, and 37%, respectively, over $SrFeO_{3-\delta}$.

Previously, we characterized and reported the BaO- and BaX_2 (X = F, Cl, Br)-promoted Ln_2O_3 (Ln = Ho and Y) catalysts for the ODE reaction (10–12). We detected the occurrence of ionic substitutions between Ba^{2+} and Ln^{3+} and/or X^- and O^{2-} ions in these BaO- and BaX_2-modified rare earth oxide catalysts. Lattice defects generated in these catalysts, such as trapped electrons and charge-deficient oxygen, are favorable for the activation of gaseous oxygen molecules, a key step in the conversion of C_2H_6 to C_2H_4. We also found that the addition of halides to the rare earth oxides could reduce the deep oxidation of C_2H_6 and C_2H_4.

Perovskite-type oxides, ABO_3, are chemically and mechanically stable. They may provide a surface with large oxygen capacity for oxidative reactions (13, 14). In these materials, the substitution of A- and/or B-site cations with foreign metal cations would give rise to the modification of catalytic properties. Doping with lower-valence cations to the A site would result either in an increase in the oxidation states of B-site cations or in the formation of oxygen vacancies (15). For instance, with an increase in strontium content, the catalytic performance of $La_{1-x}Sr_xMO_{3-\delta}$ (M = Co, Cr, Fe, Mn) perovskites increased for the CO oxidation reaction (16, 17). Oxygen vacancies and the coexistence of multivalent B-site cations induced by A-site substitution played important roles in the complete oxidation of ammonia (15), carbon monoxide (16–18), and hydrocarbons (19). We envisage that by embedding halide ions in the lattice of perovskite-type oxides, we could convert these deep

[1] To whom correspondence should be addressed. Fax: (852) 2339–7348. E-mail: pctau@hkbu.edu.hk.

0021-9517/00 $35.00

oxidation materials to selective catalysts for the ODE reaction. Putting the idea into practice, we have designed and prepared a novel class of halide-incorporated perovskite-type oxides, $La_{1-x}Sr_xB_{1-y}B'_yO_{3-\delta}X_\sigma$ (B, B' = Fe, Co, Ni, Cu, Mn; X = F, Cl; x = 0–1; y = 0–1), and found that they performed well for the oxidative dehydrogenation of ethane. In this paper, we present the catalytic performance and characterization of $La_{1-x}Sr_xFeO_{3-\delta}X_\sigma$ (X = F, Cl) and $La_{1-x}Sr_xFeO_{3-\delta}$ (for comparison purposes) catalysts for the ODE reaction.

EXPERIMENTAL

The catalysts were prepared by adopting the method of citric acid complexing (20). $La(NO_3)_3 \cdot 6H_2O$ (Sigma, >99.0%), $Sr(NO_3)_2$ (Fluka, >99%), and $Fe(NO_3)_3 \cdot 6H_2O$ (Acros, ≥99%) (for $La_{1-x}Sr_xFeO_{3-\delta}$) or LaF_3 (Acros, >99.0%; or $LaCl_3 \cdot 6H_2O$, Sigma, >99.9%), $Sr(NO_3)_2$ (Fluka, >99%), and $Fe(NO_3)_3 \cdot 6H_2O$ (Acros, ≥99%) (for $La_{1-x}Sr_xFeO_{3-\delta}X_\sigma$) were mixed in aqueous solution at the desired stoichiometric ratio. Citric acid (monohydrate, Aldrich, >99.0%) equimolar to the metals was added. The solution was then evaporated at 70°C to produce a viscous syrup. After subsequent evaporation at 100°C for 5 h and calcination at 950°C for 10 h, the material was in turn ground, pressed, crushed, and sieved to a size range of 40–80 mesh.

The activity measurement was performed at atmospheric pressure with 0.5 g of the catalyst being placed in a fixed-bed quartz microreactor (i.d. = 4 mm). The reaction temperatures ranged from 520 to 660°C at 20°C intervals. A mixture of ethane and air was passed through the microreactor. The flow rate was regulated with a mass flow controller. It was 14.8 mL min^{-1} for ethane and 35.2 mL min^{-1} for air, giving a space velocity of 6000 mL h^{-1} g^{-1} and a C_2H_6/O_2 molar ratio of 2/1. The product mixture (C_2H_6, C_2H_4, CH_4, CO, and CO_2) was determined on-line with a gas chromatograph (Shimadzu 8A TCD) with Porapak Q and 5A Molecular Sieve columns. For the variation of space velocity, the catalyst mass was varied at a fixed flow rate of 50 mL min^{-1}.

The phase compositions of the catalysts were determined with an X-ray diffractometer (XRD, D-MAX, Rigaku) operating at 40 kV and 200 mA using Cu$K\alpha$ radiation filtered with a graphite monochromator. The patterns recorded were referred to the powder diffraction files—PDF-2 Database for the identification of crystal structures. X-ray photoelectron spectroscopy (XPS, Leybold Heraeus-Shengyang SKL-12) was used to determine the O 1*s* binding energy of surface oxygen species. Before XPS measurements, the samples were calcined in O_2 (flow rate, 20 mL min^{-1}) at 850°C for 1 h and then cooled in O_2 to room temperature, followed by treatments in He (20 mL min^{-1}) at 400 and 560°C for 1 h, respectively, and then cooling in He to room temperature. The treated samples were then outgassed in the primary vacuum chamber at 10^{-5} Torr for 0.5 h and introduced into the ultrahigh vacuum chamber for recording. The C 1*s* line at 284.6 eV was taken as a reference for binding energy calibration. The specific surface areas of the catalysts were measured using a Nova 1200 apparatus.

Thermogravimetric analysis (TGA) was carried out on a thermal analyzer (Shimadzu DT-40) containing an electrobalance. The sample (10 mg) was kept in a flow of nitrogen (20 mL min^{-1}) and heated from room temperature to 900°C at the rate of 20°C min^{-1}. Before performing a TGA experiment, the sample was reduced in a 7% H_2–93% N_2 (v/v) mixture (50 mL min^{-1}) at 560°C for 0.5 h and then evacuated *in situ* at 850°C for 1 h and finally cooled in O_2 (20 mL min^{-1}) to room temperature. Such treatment was to guarantee that the adsorbed CO_2 and H_2O were removed from the sample.

For the O_2-TPD (temperature-programmed desorption) studies, the samples (0.5 g) were placed in the middle of a quartz microreactor of 4-mm i.d. The outlet gases were analyzed on-line by mass spectrometry (HP G1800A). The heating rate was 10°C min^{-1} and the temperature range was 30 to 850°C. Before an O_2-TPD experiment, the sample was evacuated *in situ* at 850°C for 1 h and then calcined at the same temperature for 1 h under an oxygen flow of 20 mL min^{-1}, followed by cooling in oxygen to room temperature and helium purging (20 mL min^{-1}) for 1 h.

Temperature-programmed reduction (TPR) was conducted by using a 7% H_2–93% N_2 (v/v) mixture. The flow rate of the carrier gas was 50 mL min^{-1} and a thermal conductivity detector was used. The amount of the sample used was 0.2 g and the heating rate was 10°C min^{-1}. Before performing a TPR experiment, the sample was first calcined *in situ* at 850°C for 1 h under an oxygen flow of 15 mL min^{-1}, followed by cooling in oxygen to room temperature.

We performed pulse experiments to investigate the reactivity of surface oxygen species. A catalyst sample (0.2 g) was placed in a microreactor and was thermally treated at a desired temperature for 30 min before the pulsing of C_2H_6 or C_2H_6/O_2 (2/1 molar ratio) and the effluent was analyzed on-line with a mass spectrometer (HP G1800A). The pulse size was 65.7 μL (at 25°C, 1 atm) and He (Hong Kong Oxygen Co., purity > 99.995%) was the carrier gas.

The procedures for analysis of fluorine and chlorine contents in the catalysts were as described previously (21). The experimental error for halide analysis is ±0.05%. The content of Fe^{3+} was determined by titrating a digested sample against potassium dichromate in HCl (3 *M*) with an excess amount of Mohr's salt (15). The experimental error for Fe^{3+} content determination is estimated to be ±1.0%.

RESULTS

Catalyst Structure, Composition, and Surface Area

Table 1 shows the crystal phases, compositions, and surface areas of the perovskite-type oxide and halo-oxide

TABLE 1

Crystal Structures, Compositions, and Surface Areas of Catalysts

Catalyst	Phase composition[a]	Fe^{4+}/Fe[b] (%)	F or Cl content (wt%)	δ	σ	Surface area ($m^2\ g^{-1}$)
$LaFeO_{3-\delta}$	O	—	—	—	—	4.40
$La_{0.8}Sr_{0.2}FeO_{3-\delta}$	O	15.8	—	0.021	—	4.34
$La_{0.6}Sr_{0.4}FeO_{3-\delta}$	O	30.5	—	0.048	—	4.06
$La_{0.4}Sr_{0.6}FeO_{3-\delta}$	O + C	45.1	—	0.075	—	4.01
$La_{0.2}Sr_{0.8}FeO_{3-\delta}$	O + C	58.0	—	0.110	—	3.92
$LaFeO_{3-\delta}F_\sigma$	O	3.1	0.95	0.045	0.122	4.20
$La_{0.8}Sr_{0.2}FeO_{3-\delta}F_\sigma$	O	21.0	1.75 1.74[c]	0.103	0.216	4.02
$La_{0.6}Sr_{0.4}FeO_{3-\delta}F_\sigma$	O	37.9	2.01	0.130	0.238	3.91
$La_{0.4}Sr_{0.6}FeO_{3-\delta}F_\sigma$	O + C	49.1	2.30	0.184	0.259	3.84
$La_{0.2}Sr_{0.8}FeO_{3-\delta}F_\sigma$	O + C	62.2	2.63	0.230	0.282	3.62
$LaFeO_{3-\delta}Cl_\sigma$	O	2.6	1.27	0.031	0.088	3.89
$La_{0.8}Sr_{0.2}FeO_{3-\delta}Cl_\sigma$	O	18.9	1.72	0.062	0.114	3.80
$La_{0.6}Sr_{0.4}FeO_{3-\delta}Cl_\sigma$	O	35.8	2.57 2.58[c]	0.103	0.164	3.74
$La_{0.4}Sr_{0.6}FeO_{3-\delta}Cl_\sigma$	O + C	47.2	3.31	0.165	0.202	2.73
$La_{0.2}Sr_{0.8}FeO_{3-\delta}Cl_\sigma$	O + C	61.1	4.38	0.223	0.256	2.29

[a] O, orthorhombic; C, cubic.
[b] Fe^{4+}/Fe ratios were calculated based on the assumption that only Fe^{3+} and Fe^{4+} ions were present in the samples.
[c] After 40 h of onstream ODE reaction.

catalysts. Based on the XRD patterns of the undoped and halide-doped perovskites (not shown), we deduced that for $La_{1-x}Sr_xFeO_{3-\delta}$ and $La_{1-x}Sr_xFeO_{3-\delta}X_\sigma$, a single-phase (orthorhombic) solid solution existed when $x \leq 0.4$, whereas two phases (orthorhombic and cubic) existed when $x \geq 0.6$. We also observed that the crystal structures of the used (after 40 h of onstream ODE reaction) $La_{0.8}Sr_{0.2}FeO_{3-0.103}F_{0.216}$ and $La_{0.6}Sr_{0.4}FeO_{3-0.103}Cl_{0.164}$ catalysts were rather similar to those of the fresh ones, respectively. From Table 1, one can realize that with the increase in x value from 0 to 0.8, Fe^{4+}/Fe ratios, halide contents, and δ and σ values increased whereas surface areas decreased. These results indicated that the substitution of Sr for La results in increases in Fe^{4+} concentration and oxygen vacancy. It was observed that the addition of F^- or Cl^- ions to $La_{1-x}Sr_xFeO_{3-\delta}$ caused the Fe^{4+} concentration to increase. The values of the four parameters, namely, Fe^{4+}/Fe ratio, δ and σ values, and surface area of the F-doped catalysts, were higher than those of the Cl-doped counterparts. One can also observe that the changes in F content at $x = 0.2$ or Cl content at $x = 0.4$ in the halide-doped perovskites before and after 40 h of onstream ODE reaction were insignificant.

Catalytic Performance

The performance of the undoped and halide-doped perovskite catalysts at 660°C is summarized in Table 2. Over $La_{1-x}Sr_xFeO_{3-\delta}$ ($x = 0.2$–0.8), with the increase in Sr content, C_2H_6 conversion increased whereas C_2H_4 selectivity and C_2H_4 yield reached maximum values of 38.8 and 21.5%, respectively, at $x = 0.4$. The behavior of $LaFeO_{3-\delta}$ was rather similar to that of $La_{0.6}Sr_{0.4}FeO_{3-0.048}$. Over $La_{1-x}Sr_xFeO_{3-\delta}F_\sigma$ ($x = 0.2$–0.8), with increasing Sr content, C_2H_6 conversion and C_2H_4 yield decreased while C_2H_4 selectivity increased. Among the F-doped catalysts;

TABLE 2

Catalytic Performance of Undoped and Halide-Doped Peroskite-Type Catalysts for the ODE Reaction under the Conditions of Temperature = 660°C and Space Velocity = 6000 mL h^{-1} g^{-1}

Catalyst	Conversion (%)	Selectivity (%)			Yield (%)
	C_2H_6	CO_x[a]	CH_4	C_2H_4	C_2H_4
Quartz sand	5.0	12.0	0	88.0	4.4
$LaFeO_{3-\delta}$	54.6	60.1	3.8	36.1	19.7
$La_{0.8}Sr_{0.2}FeO_{3-0.021}$	52.5	67.1	3.9	28.2	14.8
$La_{0.6}Sr_{0.4}FeO_{3-0.048}$	55.3	57.5	3.7	38.8	21.5
$La_{0.4}Sr_{0.6}FeO_{3-0.075}$	61.3	63.6	3.9	32.5	19.9
$La_{0.2}Sr_{0.8}FeO_{3-0.110}$	68.1	67.3	3.6	29.1	19.8
$LaFeO_{3-0.045}F_{0.122}$	70.6	50.1	6.6	43.3	30.6
$La_{0.8}Sr_{0.2}FeO_{3-0.103}F_{0.216}$	76.8	30.6	7.3	62.1	47.7
$La_{0.6}Sr_{0.4}FeO_{3-0.130}F_{0.238}$	70.6	29.2	6.6	64.2	45.3
$La_{0.4}Sr_{0.6}FeO_{3-0.184}F_{0.259}$	64.4	27.4	6.5	66.1	42.6
$La_{0.2}Sr_{0.8}FeO_{3-0.230}F_{0.282}$	58.2	23.5	7.2	69.3	40.3
$LaFeO_{3-0.031}Cl_{0.088}$	70.1	45.0	6.1	48.9	37.7
$La_{0.8}Sr_{0.2}FeO_{3-0.062}Cl_{0.114}$	73.2	39.8	7.5	52.7	38.6
$La_{0.6}Sr_{0.4}FeO_{3-0.103}Cl_{0.164}$	84.4	27.1	4.5	68.4	57.6
$La_{0.4}Sr_{0.6}FeO_{3-0.165}Cl_{0.202}$	72.7	22.3	6.6	71.1	51.7
$La_{0.2}Sr_{0.8}FeO_{3-0.223}Cl_{0.256}$	68.8	21.0	6.2	72.8	50.1

[a] $CO_x = CO + CO_2$.

$La_{0.8}Sr_{0.2}FeO_{3-0.103}F_{0.216}$ performed the best, giving 76.8% C_2H_6 conversion, 62.1% C_2H_4 selectivity, and 47.7% C_2H_4 yield; for comparison, a $LaFeO_{3-0.045}F_{0.122}$ sample showed a much lower C_2H_4 selectivity of 43.3%. Over $La_{1-x}Sr_xFeO_{3-\delta}Cl_\sigma$ ($x = 0.2$–0.8), with an increase in Sr content, C_2H_4 selectivity increased whereas C_2H_6 conversion and C_2H_4 yield reached maximum values of 84.4 and 57.6%, respectively, at $x = 0.4$; for comparison, a $LaFeO_{3-0.031}Cl_{0.088}$ sample gave a much lower C_2H_4 selectivity of 48.9%. The O_2 conversions observed over all the catalysts were 100%.

Figure 1 shows the catalytic performance of $La_{0.6}Sr_{0.4}FeO_{3-0.048}$, $La_{0.8}Sr_{0.2}FeO_{3-0.103}F_{0.216}$, and $La_{0.6}Sr_{0.4}FeO_{3-0.1013}Cl_{0.164}$ as a function of reaction temperature at a space velocity of 6000 mL h^{-1} g^{-1}. With a rise in temperature from 520 to 660°C, C_2H_6 conversions and C_2H_4 yields increased over the three catalysts (Fig. 1), C_2H_4 selectivities also increased over the first and third catalysts (Figs. 1a and 1c), whereas maximum C_2H_4 selectivity (66.4%) was obtained at 640°C over the second catalyst (Fig. 1b).

Figure 2 shows the performance of the $La_{0.8}Sr_{0.2}FeO_{3-0.103}F_{0.216}$ and $La_{0.6}Sr_{0.4}FeO_{3-0.103}Cl_{0.164}$ catalysts at 660°C as related to space velocity. Over the two catalysts, with an increase in space velocity from 4000 to 10,000 mL h^{-1} g^{-1}, C_2H_6 conversion decreased whereas C_2H_4 selectivity increased. Maximum C_2H_4 yield was reached at 6000 mL h^{-1} g^{-1} over each catalyst.

From the lifetime studies of the $La_{0.8}Sr_{0.2}FeO_{3-0.103}F_{0.216}$ and $La_{0.6}Sr_{0.4}FeO_{3-0.103}Cl_{0.164}$ catalysts at 660°C and 6000 mL h^{-1} g^{-1}, we observed that over the 40 h of on-stream ODE reaction, C_2H_6 conversions, C_2H_4 selectivities, and C_2H_4 yields changed little over the two catalysts. In other words, they are stable for the ODE reaction.

Table 3 summarizes the catalytic performance of $La_{0.8}Sr_{0.2}FeO_{3-0.103}F_{0.216}$ and $La_{0.6}Sr_{0.4}FeO_{3-0.103}Cl_{0.164}$ for the oxidation of C_2H_6 or C_2H_4 at 660°C. One can see that doping F^- or Cl^- ions into perovskite-type oxides results in a significant decrease in C_2H_4 conversion and a substantial increase in C_2H_6 conversion. This indicates that inclusion of F^- or Cl^- ions in perovskites could suppress C_2H_4 deep oxidation.

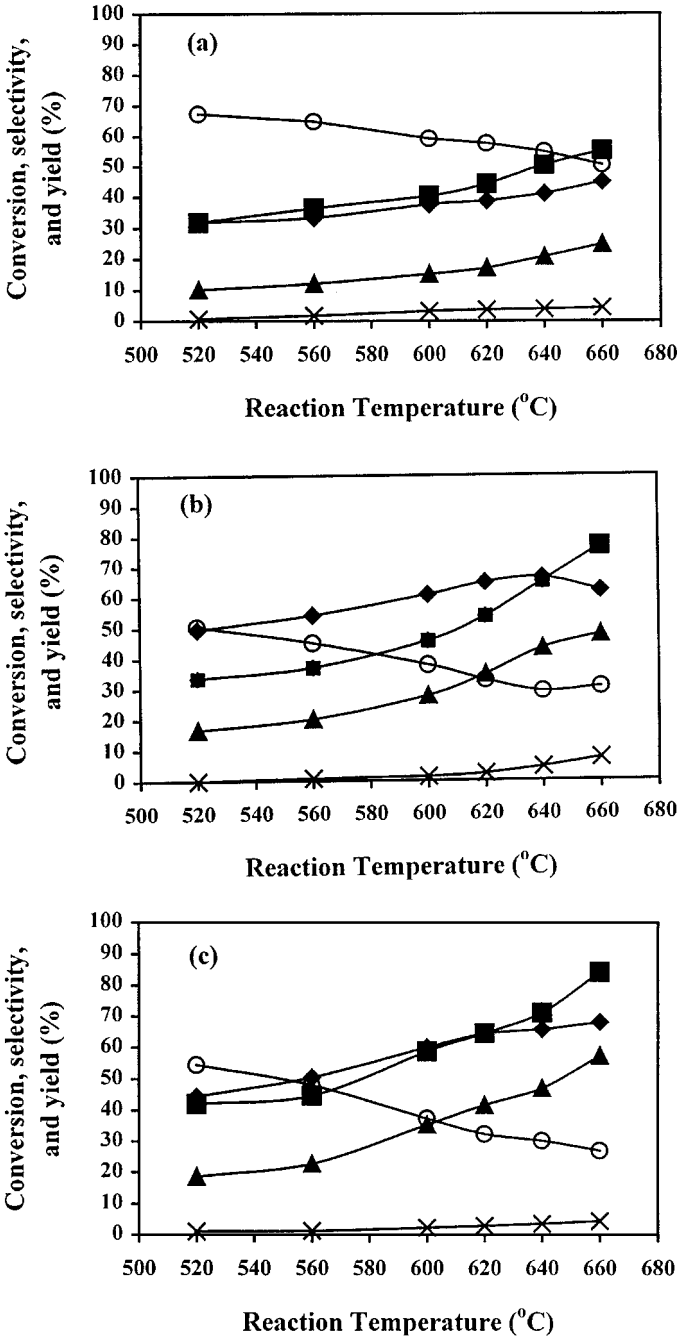

FIG. 1. Catalytic performance of (a) $La_{0.6}Sr_{0.4}FeO_{3-0.048}$, (b) $La_{0.8}Sr_{0.2}FeO_{3-0.103}F_{0.216}$, and (c) $La_{0.6}Sr_{0.4}FeO_{3-0.103}Cl_{0.164}$ as related to reaction temperature at space velocity = 6000 mL h^{-1} g^{-1}, (■) C_2H_6 conversion, (◆) C_2H_4 selectivity, (▲) C_2H_4 yield, (×) CH_4 selectivity, (○) CO_x selectivity.

TGA, XPS, O_2-TPD, and TPR Studies

Weight losses of $La_{0.6}Sr_{0.4}FeO_{3-0.048}$, $La_{0.8}Sr_{0.2}FeO_{3-0.103}F_{0.216}$, and $La_{0.6}Sr_{0.4}FeO_{3-0.103}Cl_{0.164}$ as a function of temperature are listed in Table 4. Weight losses of 0.40 and 0.12 wt% were observed in the temperature ranges 400–600 and 600–820°C, respectively, for the $La_{0.6}Sr_{0.4}FeO_{3-0.048}$ sample. A loss of 0.80 wt% was observed between 530 and 820°C for $La_{0.8}Sr_{0.2}FeO_{3-0.103}F_{0.216}$. As for the $La_{0.6}Sr_{0.4}FeO_{3-0.103}Cl_{0.164}$ sample, there was a loss of 1.30 wt% between 520 and 820°C.

Figure 3 shows the O 1*s* spectra of $La_{0.6}Sr_{0.4}FeO_{3-0.048}$, $La_{0.8}Sr_{0.2}FeO_{3-0.103}F_{0.216}$, and $La_{0.6}Sr_{0.4}FeO_{3-0.103}Cl_{0.164}$ obtained by XPS measurements. For the $La_{0.6}Sr_{0.4}FeO_{3-0.048}$ sample, there were two components at ca. 529.5 and 531.1 eV after the sample was treated in He at 400°C for 1 h (Fig. 3a). Raising the treatment temperature to 560°C removed the 531.1-eV component and left behind a 529.5-eV peak. Over the halo-oxide catalysts, two O 1*s*

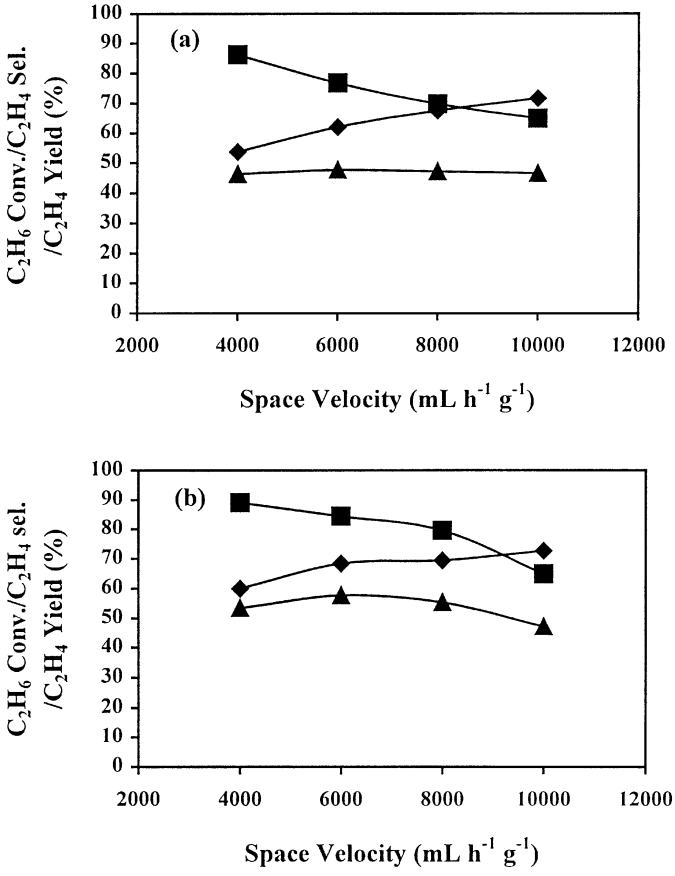

FIG. 2. Catalytic performance of (a) $La_{0.8}Sr_{0.2}FeO_{3-0.103}F_{0.216}$ and (b) $La_{0.6}Sr_{0.4}FeO_{3-0.103}Cl_{0.164}$ as related to space velocity at 660°C. (■) C_2H_6 conversion, (◆) C_2H_4 selectivity, (▲) C_2H_4 yield.

components (at ca. 530.0 and 531.2 eV for the F-doped catalyst and at ca. 530.2 and 531.4 eV for the Cl-doped catalyst) could be observed after thermal treatment at 400°C (Figs. 3b and 3c). After thermal treatment at 560°C, only the 530.1-eV component was left behind (Figs. 3b′ and 3c′). We assign the oxygen species with O 1*s* binding energy ranging from 531.0 to 531.5 eV to oxygen adsorbed at surface oxygen vacancies and/or surface hydroxyl groups; the species with O 1*s* binding energies of 529.5–530.2 eV are due to surface O^{2-} species (15, 22–26). In addition, based on the results of XPS and chemical analysis, the surface and bulk halide/oxygen ratios were estimated to be ca. 0.0751/1 and 0.0746/1 for $La_{0.8}Sr_{0.2}FeO_{3-0.103}F_{0.216}$ and 0.0573/1 and 0.0566/1 for $La_{0.6}Sr_{0.4}FeO_{3-0.103}Cl_{0.164}$, respectively.

TABLE 4

TGA Results for $La_{0.6}Sr_{0.4}FeO_{3-0.048}$, $La_{0.8}Sr_{0.2}FeO_{3-0.103}F_{0.216}$, and $La_{0.6}Sr_{0.4}FeO_{3-0.103}Cl_{0.164}$

Catalyst	Weight loss (wt%)	Temperature range (°C)
$La_{0.6}Sr_{0.4}FeO_{3-0.048}$	0.40	400–600
	0.12	600–820
$La_{0.8}Sr_{0.2}FeO_{3-0.103}F_{0.216}$	0.80	530–820
$La_{0.6}Sr_{0.4}FeO_{3-0.103}Cl_{0.164}$	1.30	520–820

Figure 4 shows the O_2-TPD profiles of $La_{0.6}Sr_{0.4}FeO_{3-0.048}$, $La_{0.8}Sr_{0.2}FeO_{3-0.103}F_{0.216}$, and $La_{0.6}Sr_{0.4}FeO_{3-0.103}Cl_{0.164}$. The profiles of used (after 40 h of ODE reaction) samples of the latter two catalysts are also shown. There were three desorption peaks in each profile. For the $La_{0.6}Sr_{0.4}FeO_{3-0.048}$ sample (Fig. 4a), the peak at ca. 505°C was the largest; the other two peaks, one stretching from ca. 600 to 750°C and the other centered at ca. 812°C, were relatively smaller. For the $La_{0.8}Sr_{0.2}FeO_{3-0.103}F_{0.216}$ sample (Fig. 4b), the first peak was at ca. 597°C, the second peak was at ca. 695°C, and there was a shoulder peak at ca. 812°C. The profiles of the fresh and used fluoro-oxide samples (Fig. 4b′) were basically the same except that the peaks obtained over the used sample showed a slight shift toward higher temperatures. As for the $La_{0.6}Sr_{0.4}FeO_{3-0.103}Cl_{0.164}$ sample (Fig. 4c), three desorption peaks appeared, respectively, at ca. 596°C, ca. 693°C, and ca. 800°C, with intensities following the order second peak > first peak > third peak; a shift in peak position toward higher temperatures was also observed over the used sample (Fig. 4c′). The similarity in the O_2-TPD profiles of fresh and used F- or Cl-doped perovskite catalysts indicates that the materials had undergone no

TABLE 3

Catalytic Performance of $La_{0.6}Sr_{0.4}FeO_{3-0.048}$, $La_{0.8}Sr_{0.2}FeO_{3-0.103}F_{0.216}$, and $La_{0.6}Sr_{0.4}FeO_{3-0.103}Cl_{0.164}$ for the Oxidation of Ethane and Ethene at Temperature = 660°C and Space Velocity = 6000 mL h^{-1} g^{-1}

	Oxidation of C_2H_4[a]		Oxidation of C_2H_6	
Catalyst	C_2H_4 conversion (%)	CO/CO_2 ratio	C_2H_6 conversion (%)	C_2H_4 selectivity (%)
$La_{0.6}Sr_{0.4}FeO_{3-0.048}$	32.3	1/11.5	55.3	45.1
$La_{0.8}Sr_{0.2}FeO_{3-0.103}F_{0.216}$	19.7	1/1.8	76.8	62.1
$La_{0.6}Sr_{0.4}FeO_{3-0.103}Cl_{0.164}$	17.8	1/1.1	84.4	68.4

[a] At $C_2H_4/O_2/N_2$ molar ratio = 2/1/3.7.

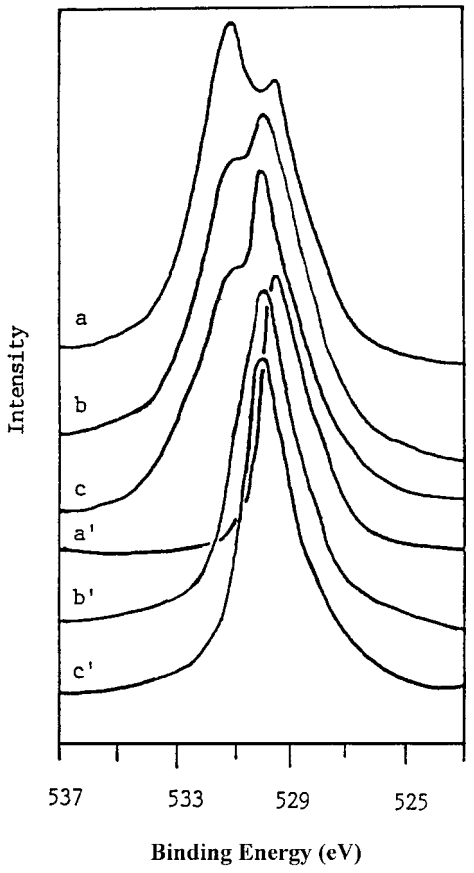

FIG. 3. X-Ray photoelectron spectra of O 1*s* for samples treated in a helium flow of 20 mL min^{-1} at 400°C for 1 h (a–c) and at 560°C for 1 h (a′–c′). (a, a′) $La_{0.6}Sr_{0.4}FeO_{3-0.048}$, (b, b′) $La_{0.8}Sr_{0.2}FeO_{3-0.103}F_{0.216}$, (c, c′) $La_{0.6}Sr_{0.4}FeO_{3-0.103}Cl_{0.164}$.

significant changes in physicochemical properties during the 40 h of ODE reaction.

Figure 5 shows the TPR profiles of the fresh $La_{0.6}Sr_{0.4}FeO_{3-0.048}$, $La_{0.8}Sr_{0.2}FeO_{3-0.103}F_{0.216}$, and $La_{0.6}Sr_{0.4}FeO_{3-0.103}Cl_{0.164}$ catalysts. For comparison, the TPR profiles of used (after 40 h of ODE reaction) samples of the latter two catalysts are also shown. For $La_{0.6}Sr_{0.4}FeO_{3-0.048}$, a large reduction peak at ca. 448°C and a broad reduction peak stretching from ca. 508 to 740°C were observed (Fig. 5a). For each of the halide-doped perovskites, there were three reduction peaks (Figs. 5b and 5c). For $La_{0.8}Sr_{0.2}FeO_{3-0.103}F_{0.216}$, the peak at ca. 665°C was the largest, that at ca. 585°C was the intermediate, and that at ca. 797°C was the smallest (Fig. 5b). For a used F-doped sample, the first two peaks shifted slightly to higher temperatures (Fig. 5b′). As for $La_{0.6}Sr_{0.4}FeO_{3-0.103}Cl_{0.164}$, the largest reduction peak was at ca. 682°C, the intermediate reduction peak at ca. 599°C, and the smallest reduction peak at ca. 790°C (Fig. 5c). For the peaks obtained over the used Cl-doped perovskite catalyst, there was a slight shift in the reduction peaks toward higher temperatures (Fig. 5c′).

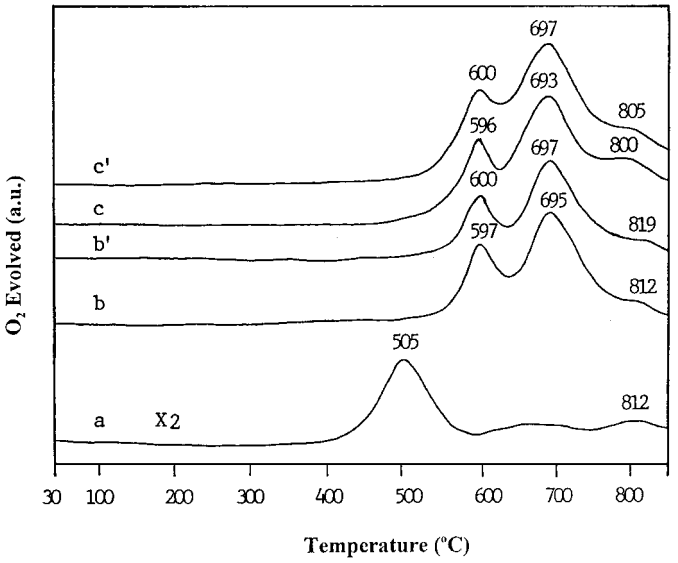

FIG. 4. O_2-TPD profiles of fresh (a–c) and used (b′, c′) (after 40 h of ODE reaction) catalysts. (a)$La_{0.6}Sr_{0.4}FeO_{3-0.048}$, (b, b′) $La_{0.8}Sr_{0.2}FeO_{3-0.103}F_{0.216}$, (c, c′) $La_{0.6}Sr_{0.4}FeO_{3-0.103}Cl_{0.164}$.

Thermal Treatment and Pulse Studies

Table 5 summarizes the changes in Fe^{4+}/Fe ratios in $La_{0.6}Sr_{0.4}FeO_{3-0.048}$, $La_{0.8}Sr_{0.2}FeO_{3-0.103}F_{0.216}$, and $La_{0.6}Sr_{0.4}FeO_{3-0.103}Cl_{0.164}$ under various thermal treatments; with a rise in temperature from 400 to 820°C in a He atmosphere, the Fe^{4+}/Fe ratio decreased from 30.2 to 23.9 mol%, 20.6 to 0.7 mol%, and 35.6 to 1.3 mol%, respectively. By exposing the treated samples to an oxygen flow of 20 mL min^{-1} at the same temperature for 30 min, the Fe^{4+}/Fe ratios were

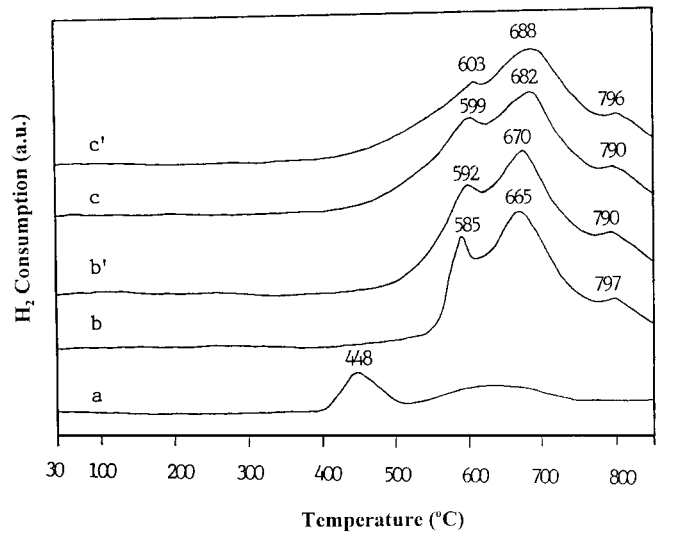

FIG. 5. TPR profiles of fresh (a–c) and used (b′, c′) (after 40 h of ODE reaction) catalysts. (a) $La_{0.6}Sr_{0.4}FeO_{3-0.048}$, (b, b′) $La_{0.8}Sr_{0.2}FeO_{3-0.103}F_{0.216}$, (c, c′) $La_{0.6}Sr_{0.4}FeO_{3-0.103}Cl_{0.164}$.

TABLE 5

Changes in Fe^{4+}/Fe Ratios in $La_{0.6}Sr_{0.4}FeO_{3-0.048}$, $La_{0.8}Sr_{0.2}FeO_{3-0.103}F_{0.216}$, and $La_{0.6}Sr_{0.4}FeO_{3-0.103}Cl_{0.164}$ after Thermal Treatments in He at Temperatures Corresponding to Oxygen Desorptions Illustrated in Fig. 4

Catalyst	Fe^{4+}/Fe ratio[a] (mol%)					Halide content[b] (wt%)	Weight loss due to the desorption of oxygen species[c] (wt%)				
	400°C	560°C	640°C	750°C	820°C	820°C	400°C	560°C	640°C	750°C	820°C
$La_{0.6}Sr_{0.4}FeO_{3-0.048}$	30.2 (30.4)[d]	25.2 (30.1)	25.0 (29.8)	24.7 (30.2)	23.9 (30.0)	—	0.01	0.38	0.40	0.42	0.48
$La_{0.8}Sr_{0.2}FeO_{3-0.103}F_{0.216}$	20.6 (20.9)	20.7 (21.1)	13.1 (19.8)	2.2 (20.4)	0.7 (21.2)	1.72	0.01	0.01	0.27	0.64	0.69
$La_{0.6}Sr_{0.4}FeO_{3-0.103}Cl_{0.164}$	35.6 (35.7)	35.2 (35.6)	27.9 (34.9)	2.1 (34.5)	1.3 (35.2)	2.56	0.01	0.02	0.28	1.19	1.22

[a] Fe^{4+}/Fe ratios were calculated according to the method stated in Table 1.
[b] Halide contents of the samples thermally treated in He at 820°C for 30 min.
[c] Weight losses were estimated based on the changes in Fe^{4+}/Fe ratio.
[d] Values in parentheses were obtained after the thermally treated sample was exposed to an oxygen flow of 20 mL min^{-1} at the same temperature for 30 min.

restored to their former values (Table 1). There was no change in halide content when the catalysts were heated in He at 820°C for 30 min. These results indicate that in an oxygen-deprived atmosphere, the drop in Fe^{4+}/Fe ratio is due to the desorption of oxygen species. Based on the Fe^{4+}/Fe ratios and the nature of oxygen desorption (Fig. 4), the weight losses due to the desorption of oxygen species were estimated and are listed in Table 5.

Table 6 summarizes C_2H_6 conversions and C_2H_4 selectivities when thermally treated $La_{0.6}Sr_{0.4}FeO_{3-0.048}$, $La_{0.8}Sr_{0.2}FeO_{3-0.103}F_{0.216}$, and $La_{0.6}Sr_{0.4}FeO_{3-0.103}Cl_{0.164}$ were exposed, respectively, to a C_2H_6 or C_2H_6/O_2 (molar ratio = 2/1) pulse at the temperature of thermal treatment. In the case of pulsing C_2H_6, with a rise in treatment temperature from 500 to 810°C, C_2H_4 selectivity increased significantly over the three catalysts; C_2H_6 conversion increased over $La_{0.6}Sr_{0.4}FeO_{3-0.048}$, whereas C_2H_6 conversion attained maximum values of 85.5 and 91.4%, respectively, over F- and Cl-doped perovskite catalysts thermally treated at 700°C. In the case of pulsing C_2H_6/O_2, with a rise in thermal treatment temperature from 500 to 810°C, C_2H_4 selectivity and C_2H_6 conversion increased considerably over the three catalysts. For comparison, we measured the activities of the three catalysts at 700°C for the reaction of ethane in the absence of oxygen at a space velocity of 6000 mL h^{-1} g^{-1}. With an increase in reaction time from 5 to 20 min, C_2H_6 conversions decreased rapidly from 10.2 to 5.6% over $La_{0.6}Sr_{0.4}FeO_{3-0.048}$, from 35.6 to 12.1% over $La_{0.8}Sr_{0.2}FeO_{3-0.103}F_{0.216}$, and from 42.4 to 15.9% over $La_{0.6}Sr_{0.4}FeO_{3-0.103}Cl_{0.164}$, respectively, whereas C_2H_4 selectivities remained at values higher than 96% over the three catalysts.

TABLE 6

Catalytic Performance of $La_{0.6}Sr_{0.4}FeO_{3-0.048}$, $La_{0.8}Sr_{0.2}FeO_{3-0.103}F_{0.216}$, and $La_{0.6}Sr_{0.4}FeO_{3-0.103}Cl_{0.164}$ in a C_2H_6 or C_2H_6/O_2 Pulse after Thermal Treatment in He at 500, 600, 700, and 810°C for 30 min

Catalyst	500°C[a]		600°C[a]		700°C[a]		810°C[a]	
	C_2H_6 conversion (%)	C_2H_4 selectivity (%)	C_2H_6 conversion (%)	C_2H_4 selectivity (%)	C_2H_6 conversion (%)	C_2H_4 selectivity (%)	C_2H_6 conversion (%)	C_2H_4 selectivity (%)
$La_{0.6}Sr_{0.4}FeO_{3-0.048}$	24.6[b] (30.2)[c]	4.2 (3.8)	31.3 (35.4)	41.1 (30.6)	32.8 (59.1)	45.2 (51.4)	40.6 (66.6)	90.8 (76.1)
$La_{0.8}Sr_{0.2}FeO_{3-0.103}F_{0.216}$	2.2 (31.1)	9.4 (50.1)	43.5 (41.6)	86.4 (61.7)	85.5 (80.2)	94.1 (81.3)	57.8 (84.6)	96.3 (87.4)
$La_{0.6}Sr_{0.4}FeO_{3-0.103}Cl_{0.164}$	1.9 (38.3)	9.8 (40.7)	59.9 (54.6)	88.2 (64.4)	91.4 (86.1)	96.6 (85.2)	64.8 (88.6)	98.2 (91.8)

[a] Temperature for thermal treatment and reactant pulsing.
[b] In a pulse of C_2H_6.
[c] The values in parentheses were obtained in a pulse of C_2H_6/O_2 (molar ratio = 2/1).

DISCUSSION

Catalytic Performance and Halide Content

From the data in Table 2, one can observe that with the introduction of halide ions into perovskites, C_2H_6 conversion and C_2H_4 selectivity increased significantly. On the basis of similar specific surface area (Table 1) and considering the best catalysts in the perovskite series, we conclude that the order of catalytic performance is $La_{0.6}Sr_{0.4}FeO_{3-0.103}Cl_{0.164} > La_{0.8}Sr_{0.2}FeO_{3-0.103}F_{0.216} \gg La_{0.6}Sr_{0.4}FeO_{3-0.048}$. With a rise in reaction temperature, C_2H_6 conversion, C_2H_4 selectivity, and C_2H_4 yield increased (Fig. 1). It is known that compared with the deep oxidation of ethane, the ODE reaction consumes a smaller amount of oxygen; at an oxygen conversion of 100%, C_2H_6 conversion and C_2H_4 selectivity could increase concurrently if ethane deep oxidation was reduced. Halide doping caused C_2H_4 conversion to decrease considerably but caused CO/CO_2 ratios to increase markedly (Table 3). This indicates that by embedding the halide ions in the $La_{1-x}Sr_xFeO_{3-\delta}$ lattice, one can reduce the deep oxidation of C_2H_4 and thus increase C_2H_4 selectivity in the ODE reaction. One should take note that the deep oxidation of C_2H_6 gives off much more heat than the ODE reaction. Over the $La_{0.8}Sr_{0.2}FeO_{3-0.103}F_{0.216}$ and $La_{0.6}Sr_{0.4}FeO_{3-0.103}Cl_{0.164}$ catalysts, with an increase in space velocity, C_2H_6 conversion decreased whereas C_2H_4 selectivity increased (Fig. 2). Similar results were observed over the three catalysts well dispersed in quartz sand (0.5 g catalyst/5.0 g quartz sand) under the same conditions, implying that the occurrence of hot spots on catalyst surfaces is not significant. In other words, the good performance observed is a result of real catalysis of the F- or Cl-doped perovskite material.

From Table 2, one sees that for the $La_{1-x}Sr_xFeO_{3-\delta}$ series, C_2H_6 conversion increased with an increase in oxygen vacancy density induced by the substitution of strontium for lanthanum. The rise in oxygen vacancy density has been suggested to be beneficial for the deep oxidation of hydrocarbons (19). For the $La_{1-x}Sr_xFeO_{3-\delta}F_\sigma$ and $La_{1-x}Sr_xFeO_{3-\delta}Cl_\sigma$ catalysts, the halide ions could replace some of the O^{2-} ions or occupy oxygen vacancies. As shown in Fig. 6(I), if a F^- or Cl^- ion replaces an O^{2-} ion, to maintain electrical neutrality, the oxidation state of an adjacent iron cation has to drop from Fe^{4+} to Fe^{3+}; if a halide ion occupies an oxygen vacancy [Fig. 6(II)], it would cause the oxidation state of an adjacent iron cation to rise from Fe^{3+} to Fe^{4+}. From Table 1, one may observe that the introduction of F^- or Cl^- ions into $La_{1-x}Sr_xFeO_{3-\delta}$ caused Fe^{4+}/Fe ratios to increase rather than to decrease, demonstrating that the halide ions have occupied a certain amount of oxygen vacancies in the form of Fig. 6(II).

With an increase in the extent of Sr/La substitution, the density of oxygen vacancies increased and C_2H_6 conversion also increased whereas C_2H_4 selectivity reached a maximum over the halide-free perovskite catalyst with $x = 0.4$ (Table 1). In the case of the halide-doped perovskites, as more oxygen vacancies were generated due to Sr substitution, more halide ions entered the oxygen vacancies and there was an increase in the Fe^{4+}/Fe ratio. C_2H_4 selectivity increased with augmentation of the σ value, whereas C_2H_6 conversion reached maximum values of 76.8 and 84.4%, respectively, over F- and Cl-doped perovskite catalysts (Table 1). That the rise in oxygen vacancy density facilitates the total oxidation of hydrocarbons and the rise in hypervalent *B*-site cation concentration is beneficial for the selective oxidation of hydrocarbons are known (15, 19). The adjustment of these two opposite effects would generate a perovskite material with the amount of oxygen vacancies and hypervalent *B*-site cations regulated for optimal catalytic performance. By comparing the activity data in Table 2 with the δ and σ values as well as the Fe^{4+}/Fe ratios in Table 1, one may detect that the best-performing catalyst in each of the three perovskite series exhibits a specific bulk density of oxygen vacancies and a particular Fe^{4+}/Fe ratio. Therefore, we suggest that the inclusion of F^- or Cl^- ions in the lattice has led to a decrease in the bulk density of oxygen vacancies and complete oxidation reactions are reduced as a result.

Since the bulk and surface halide/oxygen ratios of the halo-oxide catalysts are rather similar, we deduce that the distributions of halogen on the surface and in the bulk of the two catalysts are basically uniform. The existence of a single-phase orthorhombic perovskite $La_{0.8}Sr_{0.2}FeO_{3-0.103}F_{0.216}$ or $La_{0.6}Sr_{0.4}FeO_{3-0.103}Cl_{0.164}$ (Table 1) means that the

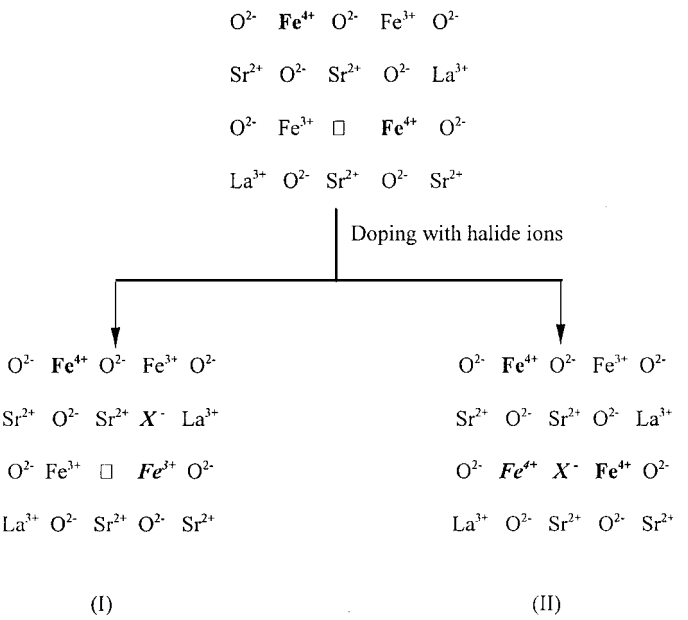

FIG. 6. Schemataic models of defects in $La_{1-x}Sr_xFeO_{3-\delta}X_\sigma$ ($X = F$, Cl): (I) X^- replacing a lattice O^{2-} ion, (II) X^- occupying an oxygen vacancy (□).

two substances are thermally stable. Furthermore, there were no significant differences in XRD patterns between the fresh and used samples (not shown). The halogen contents of the fresh and used (after 40 h of ODE reaction) catalysts were rather similar (Table 1). Lifetime studies demonstrated that the halo-oxide catalysts were stable within a period of 40 h. These results suggested that both $La_{0.8}Sr_{0.2}FeO_{3-0.103}F_{0.216}$ and $La_{0.6}Sr_{0.4}FeO_{3-0.103}Cl_{0.164}$ are good and durable catalysts for the ODE reaction.

Active Oxygen Species

Over perovskite-type oxide catalysts, oxygen molecules can be adsorbed readily to form surface oxygen species such as O_2^-, O_2^{2-}, and O^-. Most researchers believe that O^- is the active species for the complete oxidation of carbon monoxide and hydrocarbons, and O^{2-} in the lattice is responsible for the selective oxidation of these substances (18, 19, 27, 28). In the ODE or OCM reaction, however, dioxygen species such as $O_2^{\delta-}$ $(0 < \delta < 1)$, O_2^-, O_2^{n-} $(1 < n < 2)$, and O_2^- (4, 10–12, 29–32) are reported to be selective for ethene or C_{2+} product generation, whereas monoxygen species such as O^- are thought to be more prone to induce total oxidation of ethane (12, 33). Obviously, the kinds of oxygen adspecies and their distribution over the catalyst surfaces have a direct influence on catalytic performance. For ABO_3 perovskite materials, the increase in oxygen vacancies would facilitate the adsorption of gaseous oxygen molecules. The redox ability of *B*-site ions can be determined by the oxidation states of the *B*-site cations. The relative concentration of *B*-site cations with various oxidation states can also influence the catalytic behavior of the perovskites. For example, the increase in Fe^{4+}/Fe ratio in $La_{1-x}Sr_xFeO_3$ $(x = 0–1)$ is favorable to the generation of oxygen adspecies (15). If one could modify perovskite materials to give a suitable concentration of oxygen vacancies and a desired ratio of *B*-site cations, high C_2H_4 selectivity should result.

After analyzing the products formed on exposing UV-irradiated V_2O_5/SiO_2 or TiO_2 to C_2H_6, Kaliaguine *et al.* (34) pointed out that the reaction of O^- species with C_2H_6 did not result in the formation of C_2H_4. Aika and Lunsford (35) suggested that O^- species on MgO functioned as an agent for abstracting a hydrogen atom from C_2H_6 to give the ethyl radical. Although not observed experimentally, such an intermediate was suggested to react with O^{2-} species on MgO to give surface ethoxide ($C_2H_5O^-$) or to lose another hydrogen atom to generate a small amount of C_2H_4 at 25°C. Subsequent decomposition of ethoxide above 300°C produced a larger amount of C_2H_4. Based on investigations on various oxygen species formed on MgO-based catalysts (35–39), Lunsford *et al.* concluded that the reactivity of various oxygen species with hydrocarbons follows the order $O^- \gg O_3^- \gg O_2^{2-} > O_2^- > O^{2-}$. It is generally accepted that in the conversion of hydrocarbons, O^- species foment total oxidation whereas O^{2-} species induce selective oxidation (27, 28, 40).

It is well known that α and β desorption peaks are characteristic of O_2-TPD chromatograms of most perovskites. The former is due to oxygen accommodated in oxygen vacancies (19, 41); this dissociatively adsorbed oxygen is believed to be responsible for the complete oxidation of hydrocarbons (27, 28). As for β desorption, the oxygen can be associated with the partial reduction of *B*-site cations by lattice oxygen (19), and such oxygen is reckoned to be responsible for the selective oxidation of hydrocarbons (27, 28). Substitution of Sr for La leads to an increase in oxygen vacancies, thus increasing the amount of α-oxygen and strengthening the ability for complete oxidation. The rise in C_2H_6 conversion and the drop in C_2H_4 selectivity with the increase in *x* value over Sr-substituted perovskite catalysts (Table 2) are evidence supporting this viewpoint. However, with the introduction of halide ions into $La_{1-x}Sr_xFeO_{3-\delta}$, the drop in oxygen vacancy density (due to occupation by halide ions) means a decrease in α-oxygen [this was confirmed by the fact that the amount of α-oxygen adsorbed on the surface of $La_{0.8}Sr_{0.2}FeO_{3-0.103}F_{0.216}$ and $La_{0.6}Sr_{0.4}FeO_{3-0.103}Cl_{0.164}$ was much less than that on $La_{0.6}Sr_{0.4}FeO_{3-0.048}$ (Fig. 3)] and an increase in selective oxidation ability. From the XPS results, one realizes that the O 1*s* binding energy (ca. 530.0 eV) of lattice oxygen in $La_{0.8}Sr_{0.2}FeO_{3-0.103}F_{0.216}$ and $La_{0.6}Sr_{0.4}FeO_{3-0.103}Cl_{0.164}$ was ca. 0.5 eV higher than that (529.5 eV) of $La_{0.6}Sr_{0.4}FeO_{3-0.048}$ (Fig. 3), indicating that the bonds between *A*- or *B*-site cations and O^{2-} ions are weakened. Due to the electronegativity of F(4.0) and Cl(3.0) (42), inclusion of F or Cl in $La_{1-x}Sr_xFeO_{3-\delta}$ would cause the valence electron density of O^{2-} to decrease and the O 1*s* binding energy of O^{2-} to increase (Fig. 3). This means that the presence of F or Cl in the ABO_3 lattice would weaken the *A*- and *B*-site cation–oxygen bonds, making the lattice oxygen more active. Since Cl^- ions (radius, 181 Å) are larger than O^{2-} ions (radius, 1.40 Å), fixing Cl^- ions in $La_{1-x}Sr_xFeO_{3-\delta}$ would cause the crystal lattice to enlarge. (Based on the XRD results, the lattice parameters, *a*, *b*, and *c*, were estimated to be, respectively, 5.533, 5.554, and 7.834 Å for $La_{0.6}Sr_{0.4}FeO_{3-0.048}$ and 5.567, 5.576, and 7.865 Å for $La_{0.6}Sr_{0.4}FeO_{3-0.103}Cl_{0.164}$.) That means the introduction of Cl^- ions would weaken the coulombic force between *A*- or *B*-site cation and O^{2-} ion. As a result, the mobility of lattice O^{2-} increased. In other words, the inclusion of F^- or Cl^- ions in $La_{1-x}Sr_xFeO_3$ enhances the mobility of lattice oxygen. The increase in C_2H_4 selectivity over halide-doped perovskite catalysts (Table 2) is supporting evidence for this point.

As halide leaching was insignificant (Tables 1 and 5), we consider that the weight losses observed in TGA studies were due to the desorption of oxygen species. From Table 4, one may ascribe the weight loss between 400 and 600°C to the desorption of α-oxygen (19) according to the reaction

$$Fe^{4+} + O^{-}_{vacancy} \rightarrow Fe^{3+} + \tfrac{1}{2}O_2, \quad [1]$$

and those between 520 and 820°C to the desorption of lattice (β) oxygen (15) according to the reaction

$$2Fe^{4+} + O^{2-}_{lattice} \rightarrow Fe^{3+} + \tfrac{1}{2}O_2. \quad [2]$$

If all the Fe^{4+} ions in $La_{0.6}Sr_{0.4}FeO_{3-0.048}$, $La_{0.8}Sr_{0.2}FeO_{3-0.103}F_{0.216}$, and $La_{0.6}Sr_{0.4}FeO_{3-0.103}Cl_{0.164}$ were reduced to Fe^{3+} and all the oxygen vacancies were occupied by dissociatively adsorbed oxygen, the weight losses due to the desorption of β-oxygen would be 1.10, 0.75, and 1.27 wt%, respectively; that due to the desorption of α-oxygen would be 0.40 wt% for the first catalyst. Obviously, the weight losses in the halo-oxide catalysts were quite close to the predicted values, whereas for the first catalyst, although the weight loss of 0.40 wt% between 400 and 600°C agreed with the predicted value of α-oxygen, the weight loss of 0.12 wt% between 600 and 820°C was much less than the predicted figure (1.10 wt%) for β-oxygen, indicating that the lattice oxygen in $La_{0.6}Sr_{0.4}FeO_{3-0.048}$ was much less mobile than those in $La_{0.8}Sr_{0.2}FeO_{3-0.103}F_{0.216}$ and $La_{0.6}Sr_{0.4}FeO_{3-0.103}Cl_{0.164}$. One sees in Table 5 that in the He atmosphere, there were slight weight losses due to oxygen desorption at 400°C; most of the dissociatively adsorbed oxygen species in $La_{0.6}Sr_{0.4}FeO_{3-0.048}$ desorbed at 560°C, resulting in a weight loss of 0.38 wt%, a value rather close to the theoretical value (0.40 wt%) obtained with reaction [1]; and there was a noticeable decrease in the Fe^{4+}/Fe ratio. Between 560 and 820°C, the Fe^{4+}/Fe ratio decreased only slightly and the weight loss was 0.10 wt%. The results indicate that the majority of weight loss was due to desorption of α-oxygen and the lattice oxygen was not mobile in $La_{0.6}Sr_{0.4}FeO_{3-0.048}$. As for $La_{0.8}Sr_{0.2}FeO_{3-0.103}F_{0.216}$ and $La_{0.6}Sr_{0.4}FeO_{3-0.103}Cl_{0.164}$, however, with an increase in treatment temperature, the decreases in Fe^{4+}/Fe ratio were significant and the weight losses of 0.69 and 1.22 wt% were quite close to the values expected (0.75 and 1.27 wt%) from reaction [2], respectively. The results indicate that the introduction of F^- or Cl^- ions into $La_{1-x}Sr_xFeO_{3-\delta}$ enhances the mobility of lattice oxygen. Passing oxygen (20 mL min^{-1}) over the catalysts that had just been thermally treated in He restored the Fe^{4+}/Fe ratios to the former values (Tables 1 and 5). These results demonstrate that oxygen from the gas phase had replenished the catalysts with oxygen

$$O_2(g) \rightarrow O_2^-(ads) \rightarrow O_2^{2-}(ads) \rightarrow O^-(ads) \rightarrow O^{2-}(ads) \rightarrow O^{2-}_{lattice}. \quad [3]$$

When a C_2H_6 pulse was introduced to the three catalysts at 500°C, $La_{0.6}Sr_{0.4}FeO_{3-0.048}$ showed high C_2H_6 conversion but poor C_2H_4 selectivity, indicating that the α-oxygen species were answerable for the complete oxidation of C_2H_6 and C_2H_4. At 600 or 700°C, C_2H_6 conversion and C_2H_4 selectivity in a C_2H_6 pulse or C_2H_6/O_2 pulse increased significantly over the three catalysts, indicating that the β-oxygen species (i.e., lattice oxygen) were accountable for the selective oxidation of C_2H_6 to C_2H_4. At 810°C in a C_2H_6 pulse, C_2H_4 selectivity increased remarkably over $La_{0.6}Sr_{0.4}FeO_{3-0.048}$; whereas C_2H_6 conversion decreased greatly over the F- and Cl-doped catalysts [the small rise in C_2H_6 conversion over $La_{0.6}Sr_{0.4}FeO_{3-0.048}$ was due to the dominance of the selective oxidation reaction (11)], indicating that at 810°C and in an oxygen-deprived atmosphere, the amount of oxygen species present on/in the catalysts was limited. For the reaction of C_2H_6 at 700°C in an O_2-free atmosphere over the three catalysts, C_2H_6 conversion decreased significantly with reaction time due to the gradual consumption of β-oxygen. In a C_2H_6/O_2 pulse at 810°C, however, C_2H_6 conversion and C_2H_4 selectivity increased over the perovskite catalysts, implying that gaseous oxygen had been transformed into lattice oxygen via reaction [3] and participated in the selective oxidation of C_2H_6 to C_2H_4.

The inclusion of F^- or Cl^- ions in $La_{1-x}Sr_xFeO_{3-\delta}$ gives rise to two effects: (i) a decrease in the amount of oxygen vacancies, i.e., a decrease in α-oxygen; (ii) an increase in Fe^{4+}/Fe ratio, i.e., the promotion of β-oxygen desorption. As shown in the O_2-TPD studies, with the addition of F^- or Cl^- ions to $La_{1-x}Sr_xFeO_{3-\delta}$, the α-oxygen peak at ca. 500°C disappeared whereas the β-oxygen peak increased in intensity (Figs. 4b and 4c). There were two major desorption peaks within the range 590 to 820°C. They correspond to the lattice oxygen species whose coordination environments are different due to the inclusion of F^- or Cl^- ions in $La_{1-x}Sr_xFeO_{3-\delta}$. Such an assignment is supported by the fact that only lattice oxygen was present after the $La_{0.6}Sr_{0.4}FeO_{3-0.048}$, $La_{0.8}Sr_{0.2}FeO_{3-0.103}F_{0.216}$, and $La_{0.6}Sr_{0.4}FeO_{3-0.103}Cl_{0.164}$ samples were treated in He at 560°C for 1 h (Figs. 3a′–3c′). It is clear that the concentration and distribution of oxygen species on/in $La_{0.8}Sr_{0.2}FeO_{3-0.103}F_{0.216}$ and $La_{0.6}Sr_{0.4}FeO_{3-0.103}Cl_{0.164}$ are different from those on/in $La_{0.6}Sr_{0.4}FeO_{3-0.048}$. As shown in Table 2 and Fig. 1, $La_{0.8}Sr_{0.2}FeO_{3-0.103}F_{0.216}$ and $La_{0.6}Sr_{0.4}FeO_{3-0.103}Cl_{0.164}$ catalysts exhibited high C_2H_4 selectivities at temperatures ranging from 520 to 660°C, coinciding with the temperatures for major β-oxygen desorptions (Figs. 4b and 4c). Therefore, we suggest that the oxygen species that desorbed within the range 590–700°C are the active species for the selective oxidation of ethane.

Compared with the O_2-TPD results (Fig. 4), we know that the TPR band at ca. 448°C (Fig. 5a) and the two bands in the ranges 585–600 and 665–682°C (Figs. 5b and 5c) are due to the reduction of α- and β-oxygen species, respectively. These results indicate that after the halide ions are implanted in the perovskite lattice, the amount of α-oxygen decreases to extinction while the amount of β-oxygen increases. According to the nature of α- and

β-oxygen, one can deduce that the oxygen vacancy density decreased while the Fe^{4+}/Fe ratio rose in the halide-doped perovskite materials. This is in good agreement with the data in Table 1. The reduction temperatures (Figs. 5b and 5c) also coincide with the temperatures at which the catalysts performed well (Fig. 1). The TPR profiles of the fresh and the used samples (Figs. 5b, 5b′, 5c, and 5c′) are rather similar, indicative of good stability of the perovskite-type halo-oxide catalysts.

CONCLUSIONS

F- or Cl-doped perovskite-type mixed oxide materials are good and durable catalysts for the ODE reaction. Halide-modified $La_{1-x}Sr_xFeO_{3-\delta}X_\sigma$ catalysts performed much better than $La_{1-x}Sr_xFeO_{3-\delta}$ catalysts. This good performance was found to be associated with the defect nature induced by the introduction of halide ions into the perovskites. Under the reaction conditions—$C_2H_6/O_2/N_2 = 2/1/3.7$, reaction temperature = 660°C, space velocity = 6000 mL h^{-1} g^{-1}—$La_{0.8}Sr_{0.2}FeO_{3-0.103}F_{0.216}$ showed 76.8% C_2H_6 conversion, 62.1% C_2H_4 selectivity, and 47.7% C_2H_4 yield; $La_{0.6}Sr_{0.4}FeO_{3-0.103}Cl_{0.164}$ showed 84.4% C_2H_6 conversion, 68.4% C_2H_4 selectivity, and 57.6% C_2H_4 yield. One of the roles of the added halides is to reduce the deep oxidation of ethene. Based on the XPS, TPD, and TPR results, we conclude that lattice oxygen O^{2-} species are responsible for the selective oxidation of ethane. Implantation of F^- or Cl^- ions in $La_{1-x}Sr_xFeO_{3-\delta}$ could enhance lattice oxygen mobility and C_2H_4 selectivity. We illustrated that the regulation of oxygen vacancy density as well as the oxidation state of *B*-site cations by means of fixing halide ions in the perovskites could convert these materials into catalysts selective for the oxidative conversion of ethane to ethene.

ACKNOWLEDGMENTS

The work described above was fully supported by a grant from the Research Grants Council of the Hong Kong Administration Region, China (Project HKBU 2050/97P). H. X. Dai thanks the HKBU for a Ph.D. studentship.

REFERENCES

1. Wang, D., Rosynek, M. P., and Lunsford, J. H., *J. Catal.* **151**, 155 (1995).
2. Conway, S. J., and Lunsford, J. H., *J. Catal.* **131**, 513 (1991).
3. Kennedy, E. M., and Cant, N. W., *Appl. Catal.* **87**, 171 (1992).
4. Au, C. T., Zhou, X. P., and Wan, H. L., *Catal. Lett.* **40**, 101 (1996).
5. Erdöhelyi, A., Máté, F., and Solymosi, F., *J. Catal.* **135**, 563 (1992).
6. Erdöhelyi, A., and Solymosi, F., *J. Catal.* **129**, 497 (1991).
7. Chang, Y. F., Somorjai, G. A., and Heinemann, H., *J. Catal.* **154**, 24 (1995).
8. Hayakawa, T., Anderson, A. G., Orita, H., Shimizu, M., and Takehira, K., *Catal. Lett.* **16**, 373 (1992).
9. Yi, G. H., Hayakawa, T., Anderson, A. G., Suzuki, K., Hamakawa, S., York, A. P. E., Shimizu, M., and Takehira, K., *Catal. Lett.* **38**, 189 (1996).
10. Au, C. T., Chen, K. D., Dai, H. X., Liu, Y. W., and Ng, C. F., *Appl. Catal. A* **177**, 185 (1999).
11. Au, C. T., Chen, K. D., Dai, H. X., Liu, Y. W., Luo, J. Z., and Ng, C. F., *J. Catal.* **179**, 300 (1998).
12. Dai, H. X., Liu, Y. W., Ng, C. F., and Au, C. T., *J. Catal.* **187**, 59 (1999).
13. Seiyama, T., *Catal. Rev. Sci. Eng.* **34**, 281 (1992).
14. Shimizu, T., *Catal. Rev. Sci. Eng.* **34**, 355 (1992).
15. Wu, Y., Yu, T., Dou, B. S., Wang, C. X., Xie, X. F., Yu, Z. L., Fan, S. R., Fan, Z. R., and Wang, L. C., *J. Catal.* **120**, 88 (1989).
16. Rajadurai, S., Carberry, J. J., Li, B., and Alcock, C. B., *J. Catal.* **131**, 582 (1991).
17. Nitadori, T., Kurihara, S., and Misono, M., *J. Catal.* **98**, 221 (1986).
18. Viswanathan, B., *in* "Properties and Applications of Perovskite-Type Oxides" (L. G. Tejuca and J. L. G. Fierro, Eds.), p. 271, 1993.
19. Seiyama, T., *in* "Properties and Applications of Perovskite-Type Oxides" (L. G. Tejuca and J. L. G. Fierro, Eds.), p. 223, 1993.
20. Rojas, M. L., Fierro, J. L. G., Tejuca, L. G., and Bell, A. T., *J. Catal.* **124**, 41 (1990).
21. Au, C. T., Liu, Y. W., and Ng, C. F., *J. Catal.* **176**, 365 (1998).
22. Kulkarni, G. U., Rao, C. N. R., and Roberts, M. W., *J. Phys. Chem.* **99**, 3310 (1995).
23. Carley, A. F., Roberts, M. W., and Santra, A. K., *J. Phys. Chem. B* **101**, 9978 (1997).
24. Yamazoe, N., Teraoka, Y., and Seiyama, T., *Chem. Lett.*, 1767 (1981).
25. Fierro, J. L. G., and Tejuca, L. G., *Appl. Surf. Sci.* **27**, 453 (1987).
26. Marcos, J. A., Buitrago, R. H., and Lombardo, E. A., *J. Catal.* **105**, 95 (1987).
27. Haber, J., "Surface Properties and Catalysis by Non-metals" (J. P. Bonnelle, B. Delmon, and E. Derouane, Eds.). Reidel, Dordrecht, 1983.
28. Bielañski, A., and Haber, J., "Oxygen in Catalysis," p. 134. Marcel Dekker, New York, 1991.
29. Au, C. T., and Zhou, X. P., *J. Chem. Soc. Faraday Trans.* **92**, 1793 (1996).
30. Au, C. T., and Zhou, X. P., *J. Chem. Soc. Faraday Trans.* **93**, 485 (1997).
31. Mestl, G., Knözinger, H., and Lunsford, J. H., *Ber. Bunsenges. Phys. Chem.* **97**, 319 (1993).
32. Lunsford, J. H., Yang, X., Haller, K., Laane, J., Mestl, G., and Knözinger, H., *J. Phys. Chem.* **97**, 13810 (1993).
33. Hutchings, G. J., Scurrell, M. S., and Woodhous, J. R., *Catal. Today* **4**, 371 (1989).
34. Kaliaguine, S. L., Shelimov, B. N., and Kazansky, V. B., *J. Catal.* **55**, 384 (1978).
35. Aika, K., and Lunsford, J. H., *J. Phys. Chem.* **81**, 1393 (1977).
36. Aika, K., and Lunsford, J. H., *J. Phys. Chem.* **82**, 1794 (1978).
37. Takita, Y., and Lunsford, J. H., *J. Phys. Chem.* **83**, 683 (1979).
38. Takita, Y., Iwamoto, M., and Lunsford, J. H., *J. Phys. Chem.* **84**, 3079 (1980).
39. Iwamoto, M., and Lunsford, J. H., *J. Phys. Chem.* **84**, 1710 (1980).
40. Libre, J. M., Parbaux, Y., Grzybowska, B., Conflant, P., and Bonnelle, J. P., *Appl. Catal.* **6**, 315 (1983).
41. Zhang, H. M., Shimizu, Y., Teraoka, Y., Miura, N., and Yamazoe, N., *J. Catal.* **121**, 432 (1990).
42. Cotton, F. A., and Wilkinson, G., "Advanced Inorganic Chemistry," 3rd ed. Interscience, New York, 1972.